

Structural factors contributing to the Abl/Lyn dual inhibitory activity of 3-substituted benzamide derivatives

Tatsuya Horio,^a Tomohiro Hamasaki,^a Toshihiko Inoue,^a Tatsushi Wakayama,^a Shinsaku Itou,^a Haruna Naito,^b Tetsuo Asaki,^b Hiroki Hayase^b and Tomoko Niwa^{b,*}

^aResearch Laboratories, Nippon Shinyaku Co. Ltd., 3-14-1 Sakura, Tsukuba, Ibaraki 305-0003, Japan

^bDiscovery Research Laboratories, Nippon Shinyaku Co., Ltd., 14 Nishinosho-Monguchi-Cho, Kisshoin, Minami-ku, Kyoto 601-8550, Japan

Received 26 December 2006; revised 25 February 2007; accepted 1 March 2007

Available online 3 March 2007

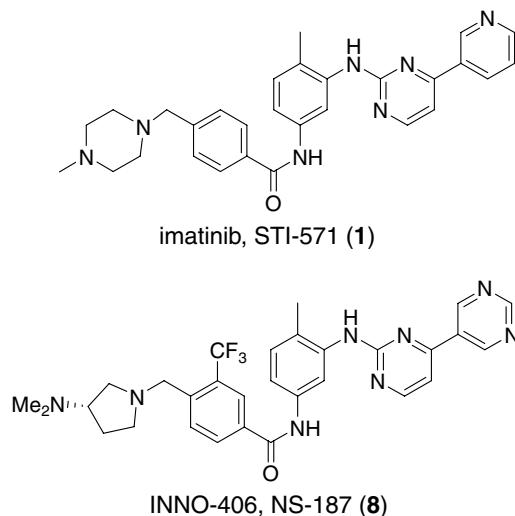
Abstract—To investigate why 3-substituted benzamide derivatives show dual inhibition of Abl and Lyn protein tyrosine kinases, we determined their inhibitory activities against Abl and Lyn, carried out molecular modeling, and conducted a structure–activity relationship study with the aid of a newly determined X-ray structure of the Abl/Lyn dual inhibitor INNO-406 (formerly known as NS-187) bound to human Abl. We found that this series of compounds interacted with both kinases in very similar ways, so that they can inhibit both kinases effectively.

© 2007 Elsevier Ltd. All rights reserved.

Chronic myeloid leukemia (CML) is caused by constitutive activation of the Bcr-Abl protein tyrosine kinase.¹ Imatinib mesylate (STI-571, Gleevec[®] or Glivec[®]; Fig. 1) inhibits the abnormal Bcr-Abl protein produced in the leukemic blood cells,^{2,3} and it is widely used to treat patients diagnosed with CML. However, resistance to imatinib has become a serious concern in imatinib therapy. Such resistance has been reported to occur through (1) point mutations in the Abl kinase domain,⁴ and (2) overexpression of Lyn kinase, a member of the Src family of tyrosine kinases.⁵

We have previously described the discovery of a series of 3-substituted benzamide derivatives with highly potent antiproliferative activity against Bcr-Abl kinase and its clinically reported mutants.^{6,7} INNO-406 (formerly known as NS-187) is one such representative compound (Fig. 1). During the course of its development, we found that INNO-406 and its derivatives also inhibited Lyn kinase. To investigate why this series of compounds acts as dual Bcr-Abl/Lyn kinase inhibitors, we determined their inhibitory activities against Abl and Lyn kinases, and studied their structure–activity relationships with

the aid of a newly determined crystal structure of the INNO-406/Abl complex and a computationally generated 3D model of the INNO-406/Lyn complex. We found that the modes of interaction of INNO-406 and its derivatives with Abl and Lyn kinases are very similar, so that these compounds can inhibit both kinases.



Keywords: Kinase; Inhibitor; Abl; Lyn; Tyrosine kinase; X-ray; Molecular modeling; QSAR.

* Corresponding author. Tel.: +81 75 321 9010; fax: +81 75 321 9038; e-mail: t.niwa@po.nippon-shinyaku.co.jp

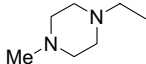
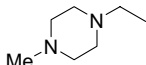
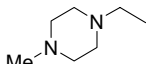
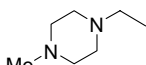
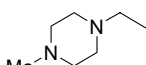
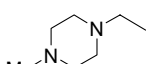
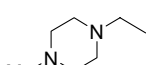
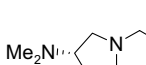
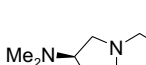
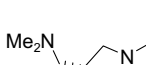
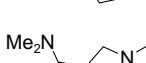
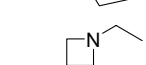
Figure 1. Chemical structures of imatinib and INNO-406.

The synthesis of the compounds has been reported elsewhere.⁷ For the Abl or Lyn kinase assay, biotinylated peptide substrates immobilized on streptavidin-coated microplates were incubated at 30 °C for 1 h with serial dilutions of the compounds in a kinase reaction buffer including 0.1 nM Lyn or 1 nM Abl. Phosphorylated peptide substrates were treated with horseradish peroxidase-conjugated anti-phosphotyrosine antibody. Tetramethylbenzidine (TMB) peroxidase substrates were then added and the absorbance at 450 nm was measured after color development. IC₅₀ values were estimated by fitting

the data to a logistic curve. The Abl kinases used for the enzyme assays and the X-ray crystallography differ at the *N*-terminus but are identical in the kinase domain, including the ligand-binding site. The differences at the *N*-terminus would not be expected to affect the results of our study.

Homology modeling, energy calculations, docking studies, and surface generation were performed with MOE 2005.06 (Chemical Computing Group, Inc.). The sequence of Lyn (LOCUS NP_002341) was aligned with

Table 1. Inhibitory and antiproliferative activity of 3-substituted benzamide derivatives

Compound	X	R ¹	R ²	IC ₅₀ (nM)		
				Lyn ^a	Abl ^a	K562 ^b
1 imatinib	CH	H		470	220	182
2	CH	F		120	35	63
3	CH	Cl		ND ^c	ND	10
4	CH	Br		12	3.1	7
5	CH	I		ND	ND	10
6	CH	CF ₃		5.1	4.8	5
7	N	CF ₃		8.8	8.5	4
8 INNO-406	N	CF ₃		26	11	11
9 ^d	N	CF ₃		12	3.4	4
10 ^d	N	CF ₃		ND	ND	11
11 ^d	N	CF ₃		32	7.6	9
12 ^d	N	CF ₃		140	29	17

^a IC₅₀ values represent the concentration of compound which inhibits the kinase activity by 50%.

^b IC₅₀ values represent the concentration of compound which inhibits cell proliferation by 50%. The data are taken from Ref. 7.

^c ND, not determined.

^d The biological activity of the monohydrochloride salts was evaluated.

that of Abl with the homology-modeling facility implemented in MOE. A set of 10 intermediate homology models was generated, and each intermediate was minimized to an energy gradient of $0.01 \text{ kcal mol}^{-1} \text{ \AA}^{-1}$. The intermediate model with the lowest energy was selected for further study. Ligands were manually docked into the binding site of Lyn by using the coordinates of the INNO-406/Abl complex as a reference. Each docked ligand and the amino acids within 7 \AA of it were then energy-minimized with the MMFF94x force field⁸ until the root-mean-square gradient of the potential energy was less than $0.05 \text{ kcal mol}^{-1} \text{ \AA}^{-1}$. Conformational changes of ligands and the nearby amino acids during minimization were small.

A recombinant baculovirus for the expression of the human c-Abl kinase domain (residues 229–515) was generated by using the Bac-to-Bac Baculovirus Expression System (Invitrogen). The kinase domain was expressed in Sf9 cells infected with the recombinant virus and purified as described elsewhere,⁹ except that INNO-406 instead of imatinib was used for complex formation with the kinase domain. The purified INNO-406/protein complex was concentrated and crystallized by the hanging-drop method at 4°C . For crystallization, the protein solution was mixed with an equal volume of reservoir solution (0.1 M MES , pH 6.0, containing $25\% \text{ PEG4000}$ and 0.3 M MgCl_2). Diffraction data from flash-frozen crystals were collected at the BL32B2 beamline of the SPring-8 synchrotron facility (Hyogo, Japan) and processed with the HKL-2000 package.¹⁶ The positions and orientations of two kinase domain monomers in the asymmetric unit were initially determined by rigid-body refinement with the program CNX (Accelrys) using a crystal structure of the kinase domain of mouse c-Abl (PDB ID code 1IEP) as a search model. Refinement with CNX and model rebuilding with the program Turbo-Frodo¹⁷ were carried out with data to 2.2 \AA resolution to a final R -factor of 0.236 and a final free R -factor of 0.270. The coordinates have been deposited in the Protein Data Bank (PDB ID code 2E2B).

All compounds tested showed more-potent inhibitory activity against Abl and Lyn than did imatinib (Table 1). The inhibitory activity of the compounds against Abl was highly correlated with their antiproliferative activity against Bcr-Abl-expressing K562 cells (correlation coefficient $r = 0.990$ when the activity is expressed as pIC_{50}) and with their inhibitory activity against Lyn ($r = 0.982$). To investigate why these compounds are highly active against both kinases, 3D structural information would be useful. We have recently solved the X-ray structure of INNO-406 bound to human Abl, shown in Figure 2a (Abl, blue; INNO-406, yellow). For comparison, the X-ray structure of imatinib bound to Abl⁹ (Abl, cyan; imatinib, white) is shown in Figure 2b. The amino acids within 4 \AA of INNO-406 or imatinib are depicted. In this and subsequent figures, the origin of the structure is shown in the upper left-hand corner as Abl (X-ray) or Lyn (model), and structures with the same origin in subsequent figures are shown in the same color. The two X-ray structures resemble each other very closely; only slight differences between

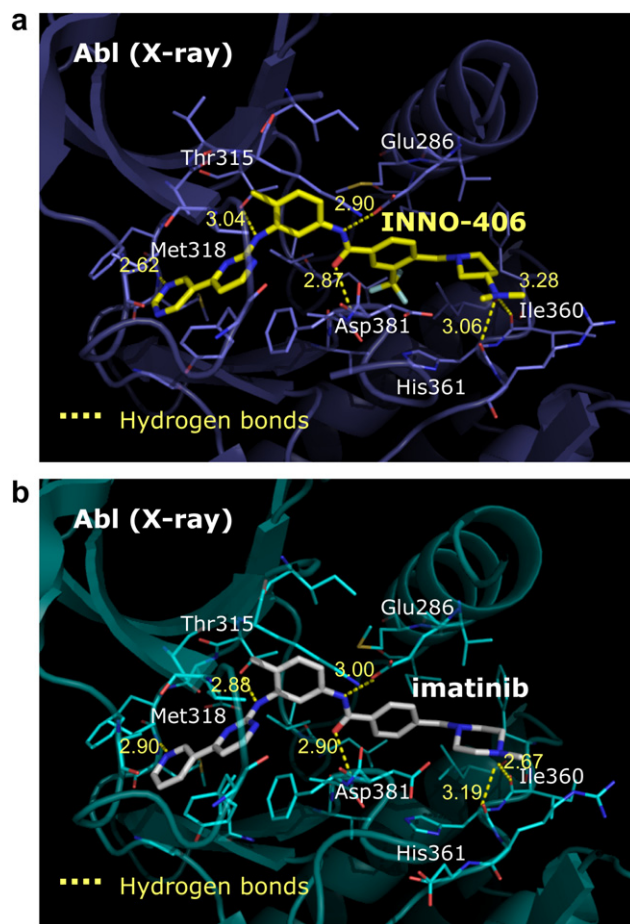


Figure 2. X-ray structures of imatinib/Abl and INNO-406/Abl complexes.

the complexes were observed in the positions of the ligands and the side chains and backbones of the kinases. It is clear that INNO-406 and imatinib interact with Abl in very similar ways.

The high sequence similarity between Abl and Lyn allowed us to construct a high-quality 3D model of Lyn by using the newly determined X-ray structure of the INNO-406/Abl complex as a template (Fig. 3). Because the inhibitory activities of 3-substituted benzamides against Abl and Lyn were highly correlated ($r = 0.982$), it is reasonable to assume that INNO-406 binds to both kinases in similar ways. On this assumption, we docked INNO-406 into the modeled structure of Lyn by using the coordinates of the INNO-406/Abl complex as a reference. An automatic docking carried out with Glide version 3.0 (Schrödinger, Inc.) produced a very similar docked structure.

The amino acids located within 4 \AA of INNO-406 in the modeled INNO-406/Lyn complex are depicted in Figure 3. The amino acids shown in white are identical in Abl and Lyn, while those shown in green differ between Abl and Lyn. For simplicity, from here on in this paper the amino acid numbering of Abl will be used for Lyn. The methyl group of the central tolyl moiety of imatinib and similar tyrosine kinase inhibitors is known as the “flag methyl”,

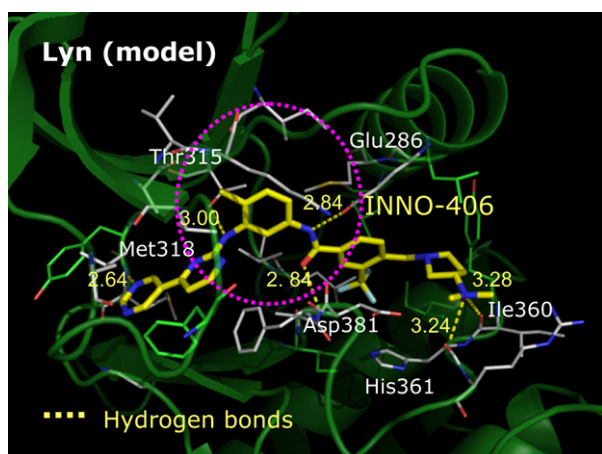


Figure 3. Binding site of the modeled structure of the INNO-406/Lyn complex. Amino acids identical in Abl and Lyn are shown in white. For simplicity, only amino acids forming hydrogen bonds with INNO-406 are labeled.

and it makes a large contribution to both their inhibitory activity and their selectivity.¹⁰ Notably, the amino acids around the tolyl moiety of INNO-406 (pink oval in Figure 3) are identical between Abl and Lyn. Other important interactions are hydrogen bonds. The amino acids of Abl that form hydrogen bonds with INNO-406 are Glu286, Thr315, Met318, Ile360, His361, and Asp381 in Abl (Fig. 2a). Among these hydrogen bonds, that between the OH group of Thr315 and the anilino NH of imatinib is reported to be critically important for the inhibitory effect of imatinib.¹¹ Identical hydrogen bonds, including one with Thr315, were found in the INNO-406/Lyn complex (Fig. 3). Thus, the critically important protein-inhibitor interactions are the same for Abl and Lyn kinases. This accounts for the potent inhibitory effect of INNO-406 and its derivatives against Lyn.

While the amino acids near the central part of INNO-406 are identical in Abl and Lyn, seven amino acids at the distal parts of the compound (labeled in Figure 4) differ between the two kinases, though the substitutions are all conservative. The five amino acids shown in white are those interacting with the distal pyrimidine ring. Among them, those at positions 253 and 317 differ between Abl and Lyn. However, mutation of Tyr253 to Phe does not greatly affect the inhibitory activity of INNO-406 against Abl.¹² Similarly, mutation of Phe317 to Leu or Val does not affect the inhibitory activity of imatinib against Abl.¹³ Accordingly, it is reasonable to assume that conservative changes at these positions will not greatly affect the binding of INNO-406 or its derivatives to Lyn. Structural determinants for the selectivity of INNO-406 against other tyrosine kinases are described elsewhere.⁶

We have previously studied the effect of 3-substituents (R^1 in Table 1) on the antiproliferative activity of 3-benzamides against Bcr-Abl-expressing K562 cells and found that the hydrophobic and steric effects of 3-substituents played important roles in enhancing the activity.⁷ In that study, the hydrophobic effect was expressed as the hydrophobic substituent parameter

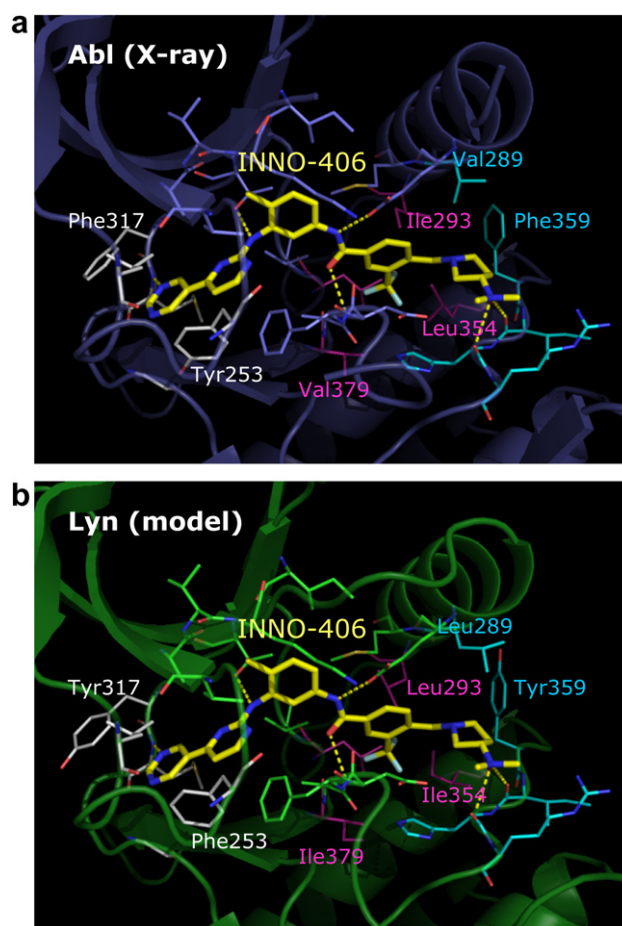


Figure 4. Binding sites of experimentally determined INNO-406/Abl (a) and modeled INNO-406/Lyn (b) structures. The labeled amino acids differ between Abl and Lyn. The amino acids around the distal pyrimidine group, R^1 , and R^2 are shown in white, magenta, and cyan, respectively.

π^{14} (H, 0.00; F, 0.14; Br, 0.86; CF_3 , 0.88), which is derived from the 1-octanol/water partition coefficients (log P) of 1-substituted benzenes, and the steric effect was expressed as Sterimol B1 (H, 1.00; F, 1.35; Br, 1.95; CF_3 , 1.99), which represents the minimum width of a substituent.¹⁵ We quantitatively analyzed the effect of the 3-substituents of 1–6 on their inhibitory activity and formulated the correlation equations 1–4:

$$pIC_{50}(\text{Abl}) = 1.753(\pm 1.602)\pi - 2.089(\pm 0.992) \quad (1)$$

$$n = 4, s = 0.300, r = 0.958, F = 22.2$$

$$pIC_{50}(\text{Lyn}) = 1.894(\pm 1.254)\pi - 2.525(\pm 0.777) \quad (2)$$

$$n = 4, s = 0.235, r = 0.977, F = 42.2$$

$$pIC_{50}(\text{Abl}) = 1.750(\pm 0.834)B1 - 4.017(\pm 1.358) \quad (3)$$

$$n = 4, s = 0.162, r = 0.988, F = 81.4$$

$$pIC_{50}(\text{Lyn}) = 1.858(\pm 0.782)B1 - 4.556(\pm 1.272) \quad (4)$$

$$n = 4, s = 0.151, r = 0.991, F = 104.5$$

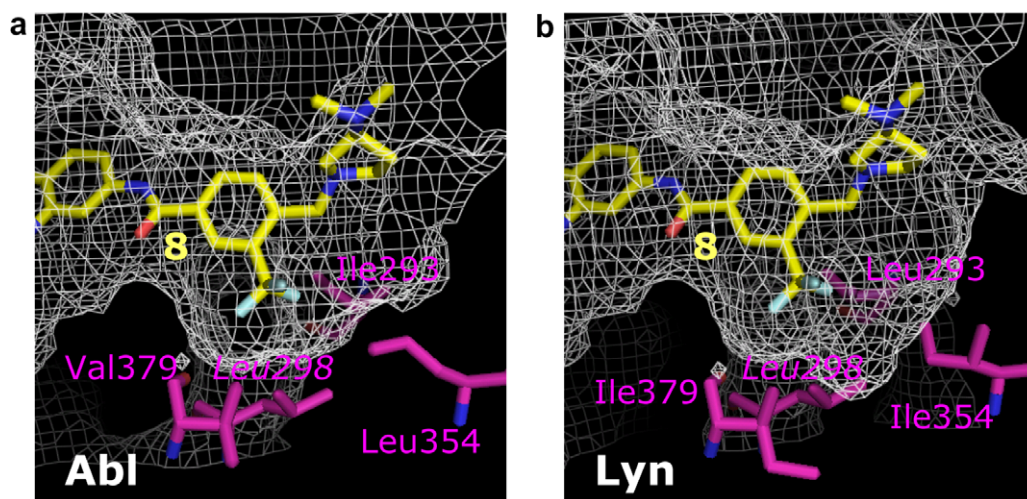


Figure 5. Mesh representation of the surfaces of Abl (a) and Lyn (b). The yellow stick structure represents compound **8**. Only the hydrophobic amino acids around the CF₃ group are depicted.

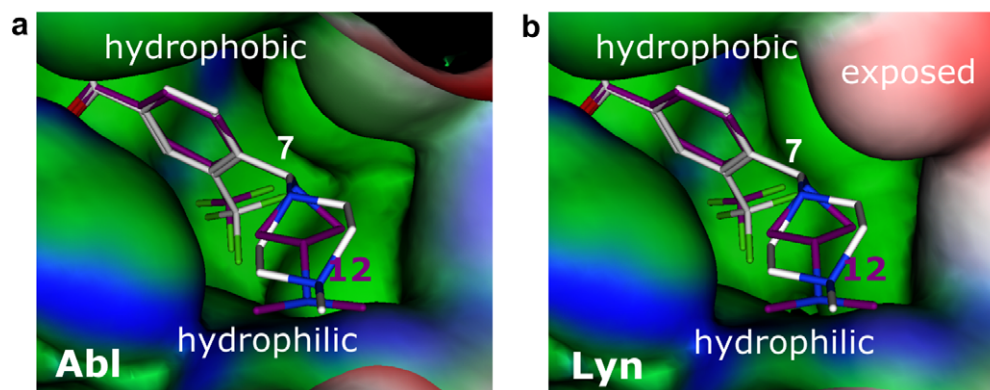


Figure 6. The surfaces of Abl (a) and Lyn (b) kinases. The white stick structure represents compound **7** and the purple stick structure represents compound **12**. Green, blue, and red indicate the hydrophobic, hydrophilic, and exposed nature of the surfaces, respectively.

In these equations, n is the number of compounds, s is the standard error, r is the correlation coefficient, F is the ratio of the variance of the calculated to that of the observed values, and the figures in parentheses are the 95% confidence intervals. Eqs. 1 and 2 indicate that the inhibitory effect increases with the hydrophobicity of R¹. Eqs. 3 and 4 show that the inhibitory effect also increases with the size of R¹. The coefficients of π and B1 agree within the 95% confidence intervals, and the statistical quality of Eqs. 1–4 is excellent. Thus, the effects of 3-substituents on the inhibition of Abl and Lyn by these compounds are very similar. These results also validate our assumption made in homology modeling that INNO-406 binds to Abl and Lyn in very similar ways.

It is of interest to study the correspondence of the findings from Eqs. 1–4 with the structural characteristics of the ligand-binding sites of the kinases. The newly determined X-ray structure of the INNO-406/Abl complex was indeed consistent with the existence of hydrophobic interactions between the 3-substituents (R¹) and the hydrophobic amino acids Ile293, Leu298, Leu354, and Val379, shown in magenta in Figure 5a. In addition,

the CF₃ group proved to occupy well the hydrophobic pocket formed by these four amino acids. The modeled structure of the INNO-406/Lyn complex is depicted in Figure 5b. Close to the 3-substituents there are four hydrophobic amino acids, Leu293, Ile379, Ile354, and Leu298, shown in magenta. Although the identities of three of the four amino acids shown in magenta differ between Abl and Lyn, they are all hydrophobic amino acids. These hydrophobic interactions thus contribute to enhance the inhibitory activity against both Abl and Lyn, and it is reasonable to suppose that the hydrophobic effect of the 3-substituent, as expressed by π , significantly increased the inhibitory activity.

Furthermore, the inhibitory activities of 1–6 were linearly correlated with Sterimol parameter B1 for the 3-substituents (Eqs. 3 and 4). Because all of the 3-substituents of 1–6 are symmetric, B1 here simply represents the width of a substituent. Since the 3-substituent is located adjacent to the R² group, its steric bulk appears to restrict the rotation of the R² group¹⁸, thereby increasing the binding affinity and hence the inhibitory activity. Presumably these two factors, the hydrophobicity and the

steric effect, work cooperatively to enhance the inhibitory activity of 3-benzamides against both Abl and Lyn.

The amino acids surrounding the 4-substituent (R^2) are shown in cyan in Figure 4. The effect of R^2 is not as simple as that of R^1 , and we could not derive significant QSAR equations for the R^2 group. Therefore, as an alternative, we examined the surface properties of the binding site in detail. The binding surfaces around R^2 generated with MOE are depicted in Figure 6. The methylpiperidine moiety of **7** occupies well the binding sites of both kinases. This corresponds to the fact that the inhibitory effects of **7** against Abl and Lyn are comparable. As the ring size of R^2 in **7**–**12** decreases, the inhibitory activity against both Abl and Lyn decreases. To investigate the reason for this trend, we docked **12** into both kinases and found that it could not fill either binding site well (Fig. 6). A weaker hydrophobic or steric interaction appears to be unfavorable for the inhibitory activity. Favorable R^2 groups are those that occupy the binding pockets well, as in **7**–**11**.

While the inhibitory effects against Abl and Lyn were comparable for the six-member- R^2 derivative **7**, the inhibitory effect against Lyn was only about one-fifth of that against Abl for the four-member- R^2 derivative **12**. The surface properties of Abl and Lyn near the R^2 group are very similar, but there are differences in the upper regions, where the binding site of Lyn is more exposed than that of Abl. These differences are due to the different natures of the amino acids at positions 289 and 359 (Fig. 4). These regions do not directly interact with the R^2 group, but they appear to have some effect on the binding affinity.

In summary, we have closely examined the binding sites of Abl and Lyn tyrosine kinases to elucidate the structure–activity relationships of a series of 3-benzamide tyrosine kinase inhibitors. Our structural studies reveal that (1) the important amino acids interacting with the tolyl group and participating in hydrogen bonding (Fig. 3) are identical in Abl and Lyn, (2) all but seven amino acids in the binding sites are identical in Abl and Lyn (Fig. 4), and (3) the seven amino acids that differ between Abl and Lyn do not greatly affect the inhibitory activity of INNO-406 (Figs. 5 and 6). These results demonstrate that appropriate selection of R^1 and R^2 for chemical modification largely contributed to the generation of inhibitors with dual activity against Abl and Lyn kinases. In addition, our molecular-modeling study showed that the R^1 and R^2 groups of INNO-406 are nearly optimal for the exhibition of high inhibitory activity against both kinases. This type of study is

expected to be of general use in the design of multiply active drugs, as well as highly selective ones.

Acknowledgment

We thank Dr. Gerald E. Smyth for helpful suggestions during the preparation of the manuscript.

References and notes

1. Deininger, M. W. N.; Goldman, J. M.; Melo, J. V. *Blood* **2000**, *96*, 3343.
2. Druker, B. J.; Tamura, S.; Buchdunger, E.; Ohno, S.; Segal, G. M.; Fanning, S.; Zimmermann, J.; Lydon, N. B. *Nat. Med.* **1996**, *2*, 561.
3. Druker, B. J.; Sawyers, C. L.; Kantarjian, H.; Resta, D. J.; Reese, S. F.; Ford, J. M.; Capdeville, R.; Talpaz, M. N. *Engl. J. Med.* **2001**, *344*, 1038.
4. Goldman, J. M.; Melo, J. V. *N. Engl. J. Med.* **2003**, *349*, 1451.
5. Donato, N. J.; Wu, J. Y.; Stapley, J.; Gallick, G.; Lin, H.; Arlinghaus, R.; Talpaz, M. *Blood* **2003**, *101*, 690.
6. Kimura, S.; Naito, H.; Segawa, H.; Kuroda, J.; Yuasa, T.; Sato, K.; Yokota, A.; Kamitsuji, Y.; Kawata, E.; Ashihara, E.; Nakaya, Y.; Naruoka, H.; Wakayama, T.; Nasu, K.; Asaki, T.; Niwa, T.; Hirabayashi, K.; Maekawa, T. *Blood* **2005**, *106*, 3948.
7. Asaki, T.; Sugiyama, Y.; Hamamoto, T.; Higashioka, M.; Umehara, M.; Naito, H.; Niwa, T. *Bioorg. Med. Chem. Lett.* **2006**, *16*, 1421.
8. Halgren, T. A. *J. Comput. Chem.* **1996**, *17*, 490.
9. Nagar, B.; Bornmann, W. G.; Pellicena, P.; Schindler, T.; Veach, D. R.; Miller, W. T.; Clarkson, B.; Kuriyan, J. *Cancer Res.* **2002**, *62*, 4236.
10. Zimmermann, J.; Buchdunger, E.; Mett, H.; Meyer, T.; Lydon, N. B. *Bioorg. Med. Chem. Lett.* **1997**, *7*, 187.
11. Schindler, T.; Bornmann, W.; Pellicena, P.; Miller, W. T.; Clarkson, B.; Kuriyan, J. *Science* **2000**, *289*, 1938.
12. Naito, H.; Kimura, S.; Nakaya, Y.; Naruoka, H.; Kimura, S.; Ito, S.; Wakayama, T.; Maekawa, T.; Hirabayashi, K. *Leukemia Res.* **2006**, *30*, 1443.
13. Burgess, M. R.; Skaggs, B. J.; Shah, N. P.; Lee, F. Y.; Sawyers, C. L. *Proc. Natl. Acad. Sci. U.S.A.* **2005**, *102*, 3395.
14. Hansch, C.; Leo, A. In *Exploring QSAR: Fundamentals and Applications in Chemistry and Biology*; American Chemical Society: Washington, DC, 1995.
15. Verloop, A. In *The STERIMOL Approach to Drug Design*; Marcel Dekker: New York, 1987.
16. Otwinowski, Z.; Minor, W. *Methods Enzymol.* **1997**, *276*, 307.
17. Roussel, A.; Cambilleau, C. In *Silicon Graphic Geometry Partners Directory*; Silicon Graphics, CA, 1989.
18. Kimura, S.; Niwa, T.; Hirabayashi, K.; Maekawa, T. *Cancer Chemother. Pharmacol.* **2006**, *58*, 55.